

# Dislocations in an arbitrary angle wedge.

## Part II: Cracks in the wedge

Journal Title  
XX(X):1–10  
©The Author(s) 0000  
Reprints and permission:  
sagepub.co.uk/journalsPermissions.nav  
DOI: 10.1177/ToBeAssigned  
www.sagepub.com/

SAGE

Daniel J. Riddoch<sup>1</sup>, Nils Cwiekala<sup>1</sup> and David A. Hills<sup>1</sup>

### Abstract

We describe a method for calculating the crack tip stress intensity factors for the problem of one or two cracks at the apex of an arbitrary angle wedge. The kernels for a dislocation in an arbitrary angle wedge described in part 1 of this paper are used extensively. Consideration is given to variations of crack length, crack angle and wedge angle.

### Keywords

dislocations, fracture mechanics, asymptotic solutions, cracks, complete contacts, wedge problems

### Introduction

A sharp-angled, semi-infinite wedge may be used to represent, the edge of a complete contact between elastically similar bodies under conditions of full adhesion, and produces a singular state of stress at the wedge's apex, whenever the contact interface remains at least locally closed<sup>1–3</sup>. Such a stress state is unsustainable, as practical materials having a finite yield strength and some plastic flow must occur to relieve the state of stress and give rise to rounding and hence a relaxation of the singularity<sup>4</sup>. The singularity may also be relaxed by frictional slip<sup>5,6</sup>, or by the development of a crack whose mouth is precisely at the edge of the contact<sup>7</sup>.

In this analysis, we will concentrate on the last of these phenomena. Cracks have long been an area of interest in applied mechanics, and many studies have examined their behaviour<sup>8,9</sup>. A cracked body behaves very differently from an uncracked body under loading. Furthermore, if left unchecked a crack in a body may continue to grow until failure occurs.

In part 1 of this paper, we discussed and developed a method for calculating the influence of a dislocation in such a system as that which we are discussing here. We will now use these results to quantify the behaviour of the tip of a crack in a semi-infinite sharp angled wedge. We recall that the faces of a crack must be traction free, and therefore, by distributing edge dislocations along the faces of a crack, we may modify the state of stress in the wedge, and determine its new value around the tip of the crack, as characterised by the crack-tip stress intensity factors. Such a system has been sketched for two particular cases in figures 1 and 5.

This method, and indeed this problem, in a very specific case, have been tackled before. Churchman and Hills<sup>7</sup> looked at the specific case of a crack in one particular location in a three quarter plane. Their paper has been found to contain a small error, and corrections are presented here along with many extensions of their work. The object of this analysis is to present calibrations for the crack tip stress intensity factors for one or two cracks in arbitrary angle wedges, the cracks themselves also being at various angles.

### Asymptotic formulation

Before we tackle the modelling of the crack, we must first consider the state of stress in the uncracked wedge. To do this, we will use the long established Williams solution<sup>10</sup>, which represents the state of stress in an asymptotic manner near the apex of the wedge. A full derivation is set out by Barber<sup>11</sup>.

The resulting solution is dominated by two eigensolutions, the mode I, or symmetric, and the mode II, or anti-symmetric, term. The stress characterised by the mode I term is singular for wedges of total internal angle greater than 180°. The stress characterised by the mode II term is singular for wedges of total internal angle greater than approximately 257°. The stress is described by the formula

$$\sigma_{ij}(r, \theta) = K_I f_{ij}^I(\theta) r^{\lambda_I - 1} + K_{II} f_{ij}^{II}(\theta) r^{\lambda_{II} - 1} \dots$$

higher order terms. (1)

where  $K_I$  and  $K_{II}$  are the mode I and mode II stress intensity factors respectively,  $\lambda_I$  and  $\lambda_{II}$  are the mode I and mode II eigenvalues respectively, and  $f_{ij}^I$  and  $f_{ij}^{II}$  are the mode I and mode II eigenvectors.

### The single crack problem

Let us now concentrate on the simplest of the many cases described above. In this section, we will consider a wedge, of total internal angle  $2\alpha$ , containing a single, straight, crack of length  $l$ , emanating from the apex of the wedge at an angle  $\phi$  from the bisector line through the wedge apex. This cracked wedge is sketched in Figure 1. The far-field load is filtered through the medium of Williams' solution, and we will assume that the cracks are sufficiently short for them to

<sup>1</sup>Department of Engineering Science, University of Oxford

#### Corresponding author:

Daniel Riddoch, Department of Engineering Science, University of Oxford, Parks Road, OX1 3PJ Oxford, United Kingdom.

Email: daniel.riddoch@eng.ox.ac.uk

experience a state of stress controlled by a hinterland given by the first two terms in a series expansion, as laid out in equation 1.

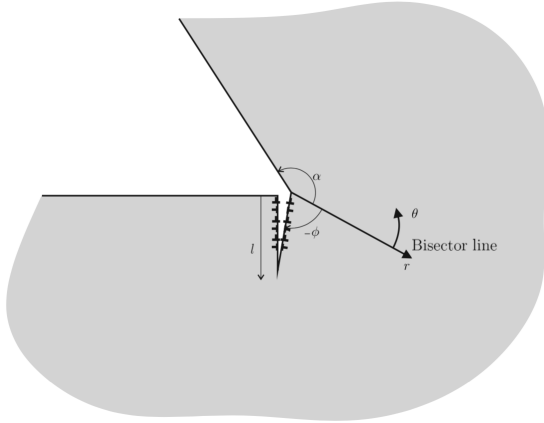


**Figure 1.** Sketch of distribution of dislocations along crack faces

### Formulation

An open crack in any circumstance will always have the property that the ‘faces’ of the crack will be free of both normal and shear traction. We will use this feature here in order to model the stresses around the crack. In order to do this, we will employ dislocations. The influence functions for these dislocations and the method of finding them is set out in part 1 of this paper.

With these functions to hand, we may proceed to distribute dislocations along the free surfaces of the crack. The state of stress induced by them must cause the tractions produced along the line of the crack in the uncracked body to vanish. The stress along this line is determined using the Williams solution, as outlined above. We can formulate the problem using integral equations.

The problem is characterised by two integral equations, and these are set out in full in . For the sake of brevity, we will display and use one only here, viz:

$$\begin{aligned}
 & -K_I f_{r\theta}^I(\phi) r^{\lambda_I-1} - K_{II} f_{r\theta}^{II}(\phi) r^{\lambda_{II}-1} = \frac{2\mu}{\pi(\kappa+1)} \dots \\
 & \int_0^l B_r(\xi) [F_{rr\theta}(r, \phi, \rho, \phi) + G_{rr\theta}(r, \phi, \rho, \phi)] + \dots \\
 & B_\theta(\xi) [F_{\theta r\theta}(r, \phi, \rho, \phi) + G_{\theta r\theta}(r, \phi, \rho, \phi)] d\xi, \dots \\
 & \text{for } 0 \leq r \leq l.
 \end{aligned} \tag{2}$$

In this formulation the influence functions are denoted by  $F_{ijk}(r, \phi, \rho, \phi)$ , and the single dislocation kernels by  $G_{ijk}(r, \phi, \rho, \phi)$ , as outlined in paper 1.  $K_I$  and  $K_{II}$  are the mode I and mode II stress intensity factors respectively, and  $\lambda_I, \lambda_{II}$  are the Williams eigenvalues, and  $f_{r\theta}^I, f_{r\theta}^{II}$  are the Williams eigenvectors,  $l$  is the length of the crack. Finally,  $\mu$  is the modulus of rigidity and  $\kappa$  is Kolosov’s constant, equal to  $3 - 4\nu$ , where  $\nu$  is Poisson’s ratio, in plane strain.

We must now solve a pair of simultaneous singular integral equations, as we did for the kernel of a dislocation in a wedge. Also as before, we will employ the Gauss-Chebyshev

quadrature, described by Erdogan et al<sup>12</sup>, with appropriate transformations. Again we wish to use the interval  $[-1, 1]$  as the integration range.

We begin by transforming the collocation points

$$r = \frac{l}{2}(v+1), \tag{3}$$

and a similar transform for the integration points

$$\xi = \frac{l}{2}(u+1). \tag{4}$$

The integration range is thus transformed. It will also prove useful to have

$$\frac{d\xi}{du} = \frac{l}{2}. \tag{5}$$

Considering the quadrature, we require the distribution of dislocations to be singular at  $u = 1$ , which represents the crack tip, but bounded at  $u = -1$ , which represents the wedge apex. Hence, we choose as the fundamental function the function  $\omega(u_j)$  having the form

$$\omega(u) = \sqrt{\frac{1+u}{1-u}}, \tag{6}$$

and so we may rewrite the dislocation densities, using the bounded function  $\varphi_i(\xi)$ , in the form

$$B_i(\xi) = \omega(\xi)\varphi_i(\xi). \tag{7}$$

We should also note the weight function for the numerical quadrature, given by

$$W(u) = \frac{2(1+u)}{2n+1}, \tag{8}$$

where  $n$  is the number of integration and collocation points in the quadrature. Having these substitutions, using the steps outlined in appendix , the integral equation can be written as

$$\begin{aligned}
 & -K_I f_{r\theta}^I(\phi) \left(\frac{l}{2}(v+1)\right)^{\lambda_I-1} - K_{II} f_{r\theta}^{II}(\phi) \left(\frac{l}{2}(v+1)\right)^{\lambda_{II}-1} \dots \\
 & = \frac{2\mu}{\pi(\kappa+1)} \int_{-1}^1 \omega_r(u) \varphi_r(u) [F_{rr\theta}(v+1, \phi, u+1, \phi) + \dots \\
 & G_{rr\theta}(v+1, \phi, u+1, \phi)] + \omega_\theta(u) \varphi_\theta(u) \dots \\
 & [F_{\theta r\theta}(v+1, \phi, u+1, \phi) + G_{\theta r\theta}(v+1, \phi, u+1, \phi)] du.
 \end{aligned} \tag{9}$$

The application of the quadrature allows us to discretise the equation as follows

$$\begin{aligned}
 & -K_I f_{r\theta}^I(\phi) \left(\frac{l}{2}(v+1)\right)^{\lambda_I-1} - K_{II} f_{r\theta}^{II}(\phi) \left(\frac{l}{2}(v+1)\right)^{\lambda_{II}-1} \dots \\
 & = \frac{2\mu}{\pi(\kappa+1)} \left[ \sum_{i=1}^n W(u_i) \varphi_r(u_i) [F_{rr\theta}(v+1, \phi, u_i+1, \phi) + \dots \right. \\
 & G_{rr\theta}(v+1, \phi, u_i+1, \phi)] + \sum_{i=1}^n W(u_i) \varphi_\theta(u_i) \dots \\
 & \left. [F_{\theta r\theta}(v+1, \phi, u_i+1, \phi) + G_{\theta r\theta}(v+1, \phi, u_i+1, \phi)] \right].
 \end{aligned} \tag{10}$$

By similar operations, the other integral equation can be similarly discretised, and as a result, we produce a system of  $2n$  simultaneous equations in  $2n$  unknowns, denoted by  $\varphi_r(u_1), \dots, \varphi_r(u_n), \varphi_\theta(u_1), \dots, \varphi_\theta(u_n)$ .

Finally, in order to determine the stress intensity factors at the crack tip which will characterise the state of stress in the neighbourhood of the crack tip, we use Krenk's interpolation<sup>13</sup>, to calculate the value of  $\varphi_r$  and  $\varphi_\theta$  at the crack tip. This then allows us to immediately calculate the stress intensity factors. The following formulae result

$$K_I^c = \frac{4\mu\sqrt{2\pi l}}{(2n+1)(\kappa+1)} \dots \sum_{i=1}^n \cot\left(\frac{\pi(2i-1)}{2(2n+1)}\right) \sin\left(\frac{n\pi(2i-1)}{2n+1}\right) \varphi_\theta(u_i), \quad (11)$$

$$K_{II}^c = \frac{4\mu\sqrt{2\pi l}}{(2n+1)(\kappa+1)} \dots \sum_{i=1}^n \cot\left(\frac{\pi(2i-1)}{2(2n+1)}\right) \sin\left(\frac{n\pi(2i-1)}{2n+1}\right) \varphi_r(u_i). \quad (12)$$

Now that the stress intensity factors may be determined, we are able to produce the following relationship,

$$\frac{1}{\sqrt{\pi l}} \begin{bmatrix} K_I^c \\ K_{II}^c \end{bmatrix} = \begin{bmatrix} a & b \\ c & d \end{bmatrix} \begin{bmatrix} K_I l^{\lambda_I-1} \\ K_{II} l^{\lambda_{II}-1} \end{bmatrix}, \quad (13)$$

where  $a, b, c, d$  are dimensionless numbers to be determined, which form a calibration between crack tip stress intensity factors and those at the wedge apex.

### The Churchman results

This problem has been previously studied by Churchman and Hills<sup>7</sup>. They considered the specific case of a crack in a three quarter plane, placed at a  $90^\circ$  angle to one of the free surfaces. That paper and several related papers formed a basis for this analysis, but it is important to note that during the course of this analysis, a small error was discovered in the original Churchman paper.

This relates to the treatment of the kernel function,  $F_{ijk}$ , in the normalisation performed from equations 11 and 12 to equations 14 and 15. In their first paper detailing these functions<sup>14</sup>, Churchman and Hills produce a function for these kernels using the single argument  $\hat{x} = \frac{x}{\xi}$ , whereas they later use two arguments,  $x$  and  $\xi$ .

This is not in itself a problem, but in changing the integration range from  $0 \leq \xi \leq c$ , to  $0 \leq \bar{\xi} \leq \bar{c}$ , the kernel function should be divided by  $d_0$ . One of the assumptions of this normalisation is that  $F_{ijk}(x, \xi) = F_{ijk}(2x, 2\xi)$ . This argument does not strictly hold. It is accurate to say that  $\bar{\sigma}_{jk}(x, \xi) = \bar{\sigma}_{jk}(px, p\xi)$ , where  $p$  is some real number and  $\bar{\sigma}_{jk}(px, p\xi) = p b_i F_{ijk}(px, p\xi)$ . Therefore  $F_{ijk}(x, \xi) = p F_{ijk}(px, p\xi)$ .

A similar mistake is again made when discretising the integral in their equations 27 and 28. Both these mistakes are minor in themselves, but nonetheless do produce a small change in the results. Churchman's results were detailed in equation 35 of their paper<sup>7</sup>, but we have recalculated them

using our method, without the errors mentioned, and the results are

$$\frac{1}{\sqrt{\pi l}} \begin{bmatrix} K_I^c \\ K_{II}^c \end{bmatrix} = \begin{bmatrix} 1.0902 & -1.1845 \\ 0.4433 & 0.4032 \end{bmatrix} \begin{bmatrix} K_I l^{\lambda_I-1} \\ K_{II} l^{\lambda_{II}-1} \end{bmatrix}. \quad (14)$$

### Generalising the angle

One of the priorities of this new analysis was to generalise the angle of the wedge and of the crack within the wedge. Previous analyses of similar problems<sup>7,15</sup> have focused on specific combinations of wedge angle and crack angle. However, our formulation is written in terms of a general angle, and the method of finding the kernels has also been done generally. So we are in a position to calculate calibration matrices such as that given in equation 14 for any combination of crack and wedge angle.

We can plot the resultant stress intensity factor ratios against the angle of the crack or the plane. Figure 2 shows how the calibration matrix entries, as defined in equation 13, vary as a crack, which is perpendicular to one of the wedge's free surfaces and has length  $l$ , is placed in a wedge of various internal half-angles, from  $\frac{\pi}{2} \leq \alpha \leq 0.97\pi$ , see figure 1 for a definition of  $\alpha$ . In this case we choose  $\phi = \frac{\pi}{2} - \alpha$ . Similarly, figure 3 shows the calibration matrix entries as the angle of the crack, set within a three quarter plane and of length 1, varies between  $-\frac{5\pi}{8} \leq \phi \leq \frac{5\pi}{8}$ , see figure 1 for a definition of  $\phi$ .

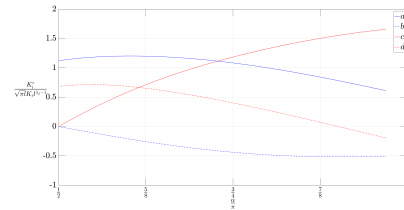


**Figure 2.** Plot of variation of stress intensity factors with changing internal wedge angle,  $2\alpha$ , and  $\phi = \frac{\pi}{2} - \alpha$ .

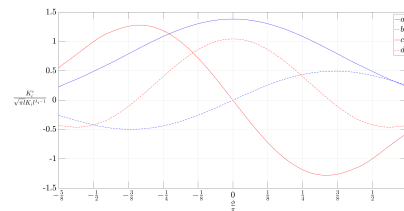


**Figure 3.** Plot of variation of stress intensity factors with changing crack angle for a three-quarter plane,  $2\alpha = \frac{3\pi}{2}$ .

### Verification

It is reasonable to want to verify these results, especially since Churchman et al compared their results to known stress intensity factors for long cracks. We present an example problem with a well known solution.

**The cracked half-plane** We consider the problem of a crack in a half-plane, subjected to remote tensile stress parallel to the free surface. This specific problem was tackled by Nowell and Hills<sup>9</sup>. They produced a clean formulation for the stress intensity factors at the tip of a crack using distributions of

dislocations along the crack face with kernels specifically calculated for a dislocation in a half-plane, and we will use their results here. Figure 4 shows an overlay of their stress intensity factor ratios (in black), with our calibrations for the same stress intensity factors overlaid (dashed, green and cyan).

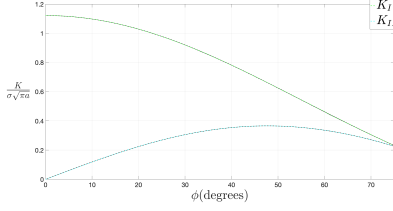


**Figure 4.** Overlay of our stress intensity factor calibrations with the results of Nowell and Hills<sup>9</sup>

An examination of figure 4 shows a good match between the calibrations. The results for angles greater than 75° are omitted, as significant numerical problems occur here with both methods. This is inevitable when using the method of distributed dislocations for producing the dislocation kernels, as lots of dislocations will be close together and have nearly parallel Burgers vectors. This will inevitably lead to numerical errors, but the fidelity of the match for angles of slant less than approximately 75° shows that the method is valid.

## The two crack problem

The problem of the single crack in the semi-infinite wedge has been tackled before and we are now able to generalise the problem in a much more comprehensive way. However, it would seem obvious to consider next how the presence of a second crack may complicate the solution. The system is sketched in figure 5

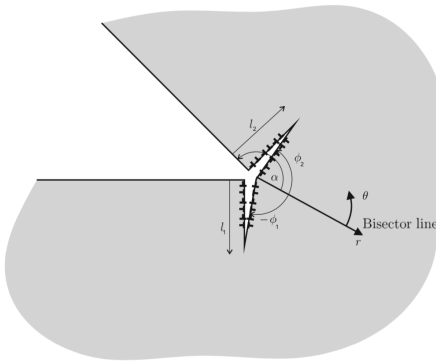


**Figure 5.** Sketch of distribution of dislocation along the faces of both cracks

Crack tips produce a singular state of stress, but we will not consider here the possibility of branching or splitting cracks, an introduction to these topics is given by Hills et al.<sup>8</sup>. Instead, we consider the possibility of another crack emanating from the notch apex. The state of stress here is still extremely high, and may result in the formation of another crack.

## Formulation

The basic approach to the two crack problem is identical to that taken to the single crack problem. Once again we will distribute dislocations along the faces of the cracks, this time we must place four distributions of dislocations, two along each crack. We will distinguish between variables relating to the cracks by the means of the subscript/superscript numerals 1 and 2.

We may proceed in much the same way, by writing the integral equations which characterise the problem. On this occasion, four integral equations are required, all of which are displayed in appendix . For the sake of brevity we will display only one, viz:

$$\begin{aligned} & \frac{2\mu}{\pi(\kappa+1)} \int_0^{l_1} B_r^1(\rho) [F_{rr\theta}(r, \phi_1, \rho, \phi_1) + G_{rr\theta}(r, \phi_1, \rho, \phi_1)] + \dots \\ & B_\theta^1(\rho) [F_{\theta r\theta}(r, \phi_1, \rho, \phi_1) + G_{\theta r\theta}(r, \phi_1, \rho, \phi_1)] d\rho + \dots \\ & \frac{2\mu}{\pi(\kappa+1)} \int_0^{l_2} B_r^2(\rho) [F_{rr\theta}(r, \phi_1, \rho, \phi_2) + G_{rr\theta}(r, \phi_1, \rho, \phi_2)] + \dots \\ & B_\theta^2(\rho) [F_{\theta r\theta}(r, \phi_1, \rho, \phi_2) + G_{\theta r\theta}(r, \phi_1, \rho, \phi_2)] d\rho \dots \\ & = -K_I f_{r\theta}^I(\phi_1) r^{\lambda_I-1} - K_{II} f_{r\theta}^{II}(\phi_1) r^{\lambda_{II}-1} \dots \\ & \text{for } 0 \leq r \leq l_1 \dots \end{aligned} \quad (15)$$

Very similar transforms are applied to those that were applied to the single crack integral equations, and these are outlined in appendix . The resulting equations are also outlined there and are characterised by equation 16, resulting from transforms of equation 15.

$$\begin{aligned} & \int_{-1}^1 \hat{B}_r^1(u) [F_{rr\theta}(v+1, \phi_1, u+1, \phi_1) + \dots \\ & G_{rr\theta}(v+1, \phi_1, u+1, \phi_1)] + \dots \\ & \hat{B}_\theta^1(u) [F_{\theta r\theta}(v+1, \phi_1, u+1, \phi_1) + \dots \\ & G_{\theta r\theta}(v+1, \phi_1, u+1, \phi_1)] du + \dots \\ & l_R \int_{-1}^1 \hat{B}_r^2(u) [F_{rr\theta}(v+1, \phi_1, l_R(u+1), \phi_2) + \dots \\ & G_{rr\theta}(v+1, \phi_1, l_R(u+1), \phi_2)] + \dots \\ & \hat{B}_\theta^2(u) [F_{\theta r\theta}(v+1, \phi_1, l_R(u+1), \phi_2) + \dots \\ & G_{\theta r\theta}(v+1, \phi_1, l_R(u+1), \phi_2)] du \dots \\ & = -K_I f_{r\theta}^I(\phi_1) \left( \frac{l_1}{2}(v+1) \right)^{\lambda_I-1} - \dots \\ & K_{II} f_{r\theta}^{II}(\phi_1) \left( \frac{l_1}{2}(v+1) \right)^{\lambda_{II}-1}, \end{aligned} \quad (16)$$

where  $l_r = \frac{l_2}{l_1}$ , and  $\hat{B}_i^j(u) = \frac{2\mu}{\pi(\kappa+1)} B_i^j(u)$ .

We use the Gauss-Chebyshev quadrature as before. Again we require the distribution to be singular at  $u = 1$ , and bounded at  $u = -1$ . So we write

$$\omega(u) = \sqrt{\frac{1+u}{1-u}}, \quad (17)$$

$$\hat{B}_i(\xi) = \omega(\xi) \hat{\varphi}_i(\xi) \quad (18)$$

$$W(u) = \frac{2(1+u)}{2n+1}, \quad (19)$$

notice that we are using the same number of points  $n$  on both cracks. So, equation 16 can be discretised to become

$$\begin{aligned}
 & \sum_{i=1}^n \hat{\varphi}_r^1(u_i) W(u_i) [F_{rr\theta}(v+1, \phi_1, u_i+1, \phi_1) + \dots \\
 & \quad G_{rr\theta}(v+1, \phi_1, u_i+1, \phi_1)] + \hat{\varphi}_\theta^1(u_i) W(u_i) \dots \\
 & \quad [F_{\theta r\theta}(v+1, \phi_1, u_i+1, \phi_1) + \dots \\
 & \quad G_{\theta r\theta}(v+1, \phi_1, u_i+1, \phi_1)] + \dots \\
 & l_R \sum_{i=1}^n \hat{\varphi}_r^2(u_i) W(u_i) [F_{rr\theta}(v+1, \phi_1, l_R(u_i+1), \phi_2) + \dots \\
 & \quad G_{rr\theta}(v+1, \phi_1, l_R(u_i+1), \phi_2)] + \dots \\
 & \quad \hat{\varphi}_\theta^2(u_i) W(u_i) [F_{\theta r\theta}(v+1, \phi_1, l_R(u_i+1), \phi_2) + \dots \\
 & \quad G_{\theta r\theta}(v+1, \phi_1, l_R(u_i+1), \phi_2)] \dots \\
 & = -K_I f_{r\theta}^I(\phi_1) \left( \frac{l_1}{2}(v+1) \right)^{\lambda_I-1} - \dots \\
 & \quad K_{II} f_{r\theta}^{II}(\phi_1) \left( \frac{l_1}{2}(v+1) \right)^{\lambda_{II}-1}. \quad (20)
 \end{aligned}$$

Krenk interpolation is once more used to determine the crack tip stress intensity factors from the solutions to the arising simultaneous equations

$$K_I^{1c} = \frac{4\mu\sqrt{2\pi l_1}}{(2n+1)(\kappa+1)l_1^{\lambda_I-1}} \dots \sum_{i=1}^n \cot\left(\frac{\pi(2i-1)}{2(2n+1)}\right) \sin\left(\frac{n\pi(2i-1)}{2n+1}\right) \varphi_\theta(u_i), \quad (21)$$

$$K_{II}^{1c} = \frac{4\mu\sqrt{2\pi l_1}}{(2n+1)(\kappa+1)l_1^{\lambda_{II}-1}} \dots \sum_{i=1}^n \cot\left(\frac{\pi(2i-1)}{2(2n+1)}\right) \sin\left(\frac{n\pi(2i-1)}{2n+1}\right) \varphi_r(u_i), \quad (22)$$

$$K_I^{2c} = \frac{4\mu\sqrt{2\pi l_2}}{(2n+1)(\kappa+1)l_2^{\lambda_I-1}} \dots \sum_{i=1}^n \cot\left(\frac{\pi(2i-1)}{2(2n+1)}\right) \sin\left(\frac{n\pi(2i-1)}{2n+1}\right) \varphi_\theta(u_i), \quad (23)$$

$$K_{II}^{2c} = \frac{4\mu\sqrt{2\pi l_2}}{(2n+1)(\kappa+1)l_2^{\lambda_{II}-1}} \dots \sum_{i=1}^n \cot\left(\frac{\pi(2i-1)}{2(2n+1)}\right) \sin\left(\frac{n\pi(2i-1)}{2n+1}\right) \varphi_r(u_i), \quad (24)$$

Now that the stress intensity factors may be determined, we are able to produce the following relationship,

$$\frac{1}{\sqrt{\pi}} \begin{bmatrix} K_I^1 l_1^{\frac{1}{\lambda_I}-\frac{1}{2}} \\ K_{II}^1 l_1^{\frac{1}{\lambda_{II}}-\frac{1}{2}} \\ K_I^2 l_2^{\frac{1}{\lambda_I}-\frac{1}{2}} \\ K_{II}^2 l_2^{\frac{1}{\lambda_{II}}-\frac{1}{2}} \end{bmatrix} = \begin{bmatrix} a & b \\ c & d \\ e & f \\ g & h \end{bmatrix} \begin{bmatrix} K_I \\ K_{II} \end{bmatrix}, \quad (25)$$

where  $a, b, c, d, e, f, g, h$  are dimensionless numbers to be determined.

### The three-quarter plane

The first example we address is the three quarter plane, with two cracks, at angles  $\pm\frac{\pi}{4}$  from the bisector. This problem can be tackled by setting  $\alpha = \frac{3\pi}{4}$ ,  $\phi_1 = \frac{\pi}{4}$ ,  $\phi_2 = -\frac{\pi}{4}$ . Then, using the method set out above the calibration for cracks of equal length, we get the following relationship:

$$\frac{1}{\sqrt{\pi}} \begin{bmatrix} K_I^1 l_1^{\frac{1}{\lambda_I}-\frac{1}{2}} \\ K_{II}^1 l_1^{\frac{1}{\lambda_{II}}-\frac{1}{2}} \\ K_I^2 l_2^{\frac{1}{\lambda_I}-\frac{1}{2}} \\ K_{II}^2 l_2^{\frac{1}{\lambda_{II}}-\frac{1}{2}} \end{bmatrix} = \begin{bmatrix} 1.0558 & -2.1207 \\ 0.7439 & 0.3416 \\ 1.0558 & 2.1207 \\ -0.7439 & 0.3416 \end{bmatrix} \begin{bmatrix} K_I \\ K_{II} \end{bmatrix}. \quad (26)$$

We may also consider the effect of varying the ratio of the length of the cracks. Figure 6 plots the variation of the coefficients of the matrix against the logarithm of the variation of the crack length ratio, note that the entries  $b, c, f$  and  $g$  are not constant, just weak functions of  $\frac{l_2}{l_1}$ .

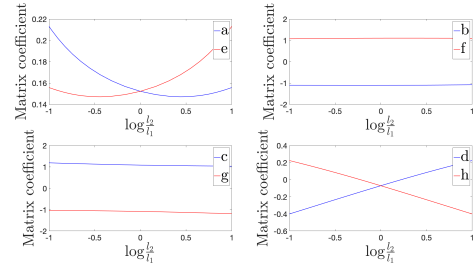


Figure 6. Plot of the coefficients of the matrix given in equation 25

### Generalising the wedge angle

Next, we consider variations of the angle of the wedge. There are infinitely many possible combinations of wedge and crack angles to consider. First, we will consider what happens if we place two cracks, one of unit length at angle  $\phi_1 = \frac{\pi}{4}$ , and a second of half-unit length at angle  $\phi_2 = -\frac{\pi}{4}$  in a three-quarter plane. Fixing these crack lengths, figure 7 shows how the matrix coefficients change as we vary the angle  $\alpha$ , the half-angle of the wedge, again note that the entries  $b, c, f$  and  $g$  are not constant, just weak functions of  $\frac{\alpha}{\pi}$ .

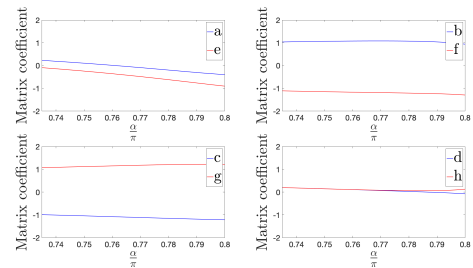
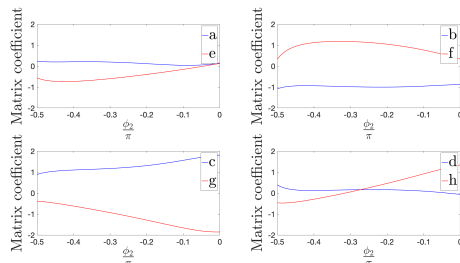


Figure 7. Plot of the coefficients of the matrix given in equation 25 as the internal wedge angle varies

## Generalising the crack angle

Alternatively, we may consider what happens if we only change the angle of one of the cracks. Figure 8 shows the variation of the matrix coefficients as the angle of one crack is varied. Specifically, we considered a three quarter plane, with one crack of unit length fixed at an angle  $\phi_1 = \frac{\pi}{4}$ , and another crack of half-unit length, whose angle is given by  $\phi_2$  and varies from  $-\frac{\pi}{2}$  to 0, or along the bisector.



**Figure 8.** Plot of the coefficients of the matrix given in equation 25 as the angle of one of the cracks varies

## Conclusions

We have described in this paper a method for evaluating the crack tip stress intensity factors for one or two cracks of arbitrary length, placed at arbitrary angles in a sharp-cornered wedge, itself of arbitrary internal angle. The method used has utilised the previously discussed kernels for a dislocation placed in such a wedge.

The results presented are verified and compared to known results for specific cases, and in the particular case discussed by Churchman and Hills<sup>14</sup>. A correction to their results is made. Furthermore, as is consistent with the objectives of this analysis, calibrations, or at least the method of finding such, are presented for cases of either one or two cracks in arbitrary angle wedges. Owing to the many possible configuration that readers may wish to investigate specifically, the MATLAB code we used to generate these results is published alongside this article.

## Acknowledgements

All authors thank Rolls-Royce plc and the EPSRC for the support under the Prosperity Partnership Grant 'Cornerstone: Mechanical Engineering Science to Enable Aero Propulsion Futures', Grant Ref: EP/R004951/1.

## References

1. Barber J. *Contact Mechanics*. Springer, 2018.
2. Johnson KL. *Contact mechanics*. Cambridge university press, 1987.
3. Dundurs J and Lee M. Stress concentration at a sharp edge in contact problems. *Journal of elasticity* 1972; 2(2): 109–112.
4. Hills DA and Dini D. Characteristics of the process zone at sharp notch roots. *International Journal of Solids and structures* 2011; 48(14-15): 2177–2183.
5. Churchman C and Hills D. Slip zone length at the edge of a complete contact. *International Journal of Solids and structures* 2006; 43(7-8): 2037–2049.
6. Paynter R, Hills D and Dini D. Separation and slip at the edge of a complete contact: An asymptotic solution. *International Journal of Solids and Structures* 2010; 47(18-19): 2613–2619.
7. Churchman C and Hills D. The edge dislocation in a three-quarter plane. part ii: Application to an edge crack. *European Journal of Mechanics-A/Solids* 2006; 25(3): 389–396.
8. Hills DA, Kelly PA, Dai DN et al. *Solution of crack problems: the distributed dislocation technique*, volume 44. Springer Science & Business Media, 2013.
9. Nowell D and Hills D. Open cracks at or near free edges. *The Journal of strain analysis for engineering design* 1987; 22(3): 177–185.
10. Williams M. Stress singularities resulting from various boundary conditions in angular corners of plates in extension. *Journal of applied mechanics* 1952; 19(4): 526–528.
11. Barber JR. *Elasticity*. Springer, 2010.
12. Erdogan F, Gupta GD and Cook T. Numerical solution of singular integral equations. In *Methods of analysis and solutions of crack problems*. Springer, 1973. pp. 368–425.
13. Krenk S. On the use of the interpolation polynomial for solutions of singular integral equations. *Quarterly of Applied Mathematics* 1975; 32(4): 479–484.
14. Churchman C, Korsunsky A and Hills D. The edge dislocation in a three-quarter plane. part i: Influence functions. *European Journal of Mechanics-A/Solids* 2006; 25(1): 42–50.
15. Philipps A, Karuppanan S, Churchman C et al. Crack tip stress intensity factors for a crack emanating from a sharp notch. *Engineering Fracture Mechanics* 2008; 75(18): 5134–5139.

## Williams solution

The solution of Williams<sup>10</sup> is well known, and produces characteristic eigenvalues and eigenvectors. In this appendix, the formulae to find the eigenvalues and eigenvectors are given, more detail is given by Barber<sup>1</sup>. The eigenvalues are the solutions of the equations

$$\lambda_I \sin(2\alpha) + \sin(2\alpha\lambda_I) = 0 \quad \& \quad \lambda_{II} \sin(2\alpha) - \sin(2\alpha\lambda_{II}) = 0. \quad (27)$$

The eigenvectors are given by

$$f_{rr}^I(\psi) = \frac{\cos[(\lambda_I - 1)\alpha]\cos[(\lambda_I + 1)\psi] - \frac{\lambda_I - 3}{\lambda_I + 1}\cos[(\lambda_I + 1)\alpha]\cos[(\lambda_I - 1)\psi]}{\cos[(\lambda_I + 1)\alpha] - \cos[(\lambda_I - 1)\alpha]} \quad (28)$$

$$f_{rr}^{II}(\psi) = \frac{\sin[(\lambda_{II} - 1)\alpha]\sin[(\lambda_{II} + 1)\psi] - \frac{\lambda_{II} - 3}{\lambda_{II} + 1}\sin[(\lambda_{II} + 1)\alpha]\sin[(\lambda_{II} - 1)\psi]}{\sin[(\lambda_{II} - 1)\alpha] - \frac{\lambda_{II} - 1}{\lambda_{II} + 1}\sin[(\lambda_{II} + 1)\alpha]} \quad (29)$$

$$f_{r\theta}^I(\psi) = \frac{\sin[(\lambda_I - 1)\alpha]\sin[(\lambda_I + 1)\psi] - \sin[(\lambda_I + 1)\alpha]\sin[(\lambda_I - 1)\psi]}{\sin[(\lambda_I - 1)\alpha] - \frac{\lambda_I + 1}{\lambda_I - 1}\sin[(\lambda_I + 1)\alpha]} \quad (30)$$

$$f_{r\theta}^{II}(\psi) = \frac{\cos[(\lambda_{II} - 1)\alpha]\cos[(\lambda_{II} + 1)\psi] - \cos[(\lambda_{II} + 1)\alpha]\cos[(\lambda_{II} - 1)\psi]}{\cos[(\lambda_{II} - 1)\alpha] - \cos[(\lambda_{II} + 1)\alpha]} \quad (31)$$

$$f_{\theta\theta}^I(\psi) = \frac{\cos[(\lambda_I - 1)\alpha]\cos[(\lambda_I + 1)\psi] - \cos[(\lambda_I + 1)\alpha]\cos[(\lambda_I - 1)\psi]}{\cos[(\lambda_I - 1)\alpha] - \cos[(\lambda_I + 1)\alpha]} \quad (32)$$

$$f_{\theta\theta}^{II}(\psi) = \frac{\sin[(\lambda_{II} - 1)\alpha]\sin[(\lambda_{II} + 1)\psi] - \sin[(\lambda_{II} + 1)\alpha]\sin[(\lambda_{II} - 1)\psi]}{-\sin[(\lambda_{II} - 1)\alpha] + \frac{\lambda_{II} - 1}{\lambda_{II} + 1}\sin[(\lambda_{II} + 1)\alpha]} \quad (33)$$

## Integral equations

### Single crack problem

$$-K_I f_{r\theta}^I(\phi) r^{\lambda_I - 1} - K_{II} f_{r\theta}^{II}(\phi) r^{\lambda_{II} - 1} = \dots$$

$$\frac{2\mu}{\pi(\kappa + 1)} \int_0^l B_r(\rho) [F_{rr\theta}(r, \phi, \rho, \phi) + G_{rr\theta}(r, \phi, \rho, \phi)] + B_\theta(\rho) [F_{\theta r\theta}(r, \phi, \rho, \phi) + G_{\theta r\theta}(r, \phi, \rho, \phi)] d\rho \quad (34)$$

$$-K_I f_{\theta\theta}^I(\phi) r^{\lambda_I - 1} - K_{II} f_{\theta\theta}^{II}(\phi) r^{\lambda_{II} - 1} = \dots$$

$$\frac{2\mu}{\pi(\kappa + 1)} \int_0^l B_r(\rho) [F_{r\theta\theta}(r, \phi, \rho, \phi) + G_{r\theta\theta}(r, \phi, \rho, \phi)] + B_\theta(\rho) [F_{\theta\theta\theta}(r, \phi, \rho, \phi) + G_{\theta\theta\theta}(r, \phi, \rho, \phi)] d\rho \quad (35)$$

### Two crack problem

$$\frac{2\mu}{\pi(\kappa + 1)} \int_0^{l_1} B_r^1(\rho) [F_{rr\theta}(r, \phi_1, \rho, \phi_1) + G_{rr\theta}(r, \phi_1, \rho, \phi_1)] + B_\theta^1(\rho) [F_{\theta r\theta}(r, \phi_1, \rho, \phi_1) + G_{\theta r\theta}(r, \phi_1, \rho, \phi_1)] d\rho + \dots$$

$$\frac{2\mu}{\pi(\kappa + 1)} \int_0^{l_2} B_r^2(\rho) [F_{rr\theta}(r, \phi_1, \rho, \phi_2) + G_{rr\theta}(r, \phi_1, \rho, \phi_2)] + B_\theta^2(\rho) [F_{\theta r\theta}(r, \phi_1, \rho, \phi_2) + G_{\theta r\theta}(r, \phi_1, \rho, \phi_2)] d\rho \dots$$

$$= -K_I f_{r\theta}^I(\phi_1) r^{\lambda_I - 1} - K_{II} f_{r\theta}^{II}(\phi_1) r^{\lambda_{II} - 1} \quad (36)$$

$$\frac{2\mu}{\pi(\kappa + 1)} \int_0^{l_1} B_r^1(\rho) [F_{r\theta\theta}(r, \phi_1, \rho, \phi_1) + G_{r\theta\theta}(r, \phi_1, \rho, \phi_1)] + B_\theta^1(\rho) [F_{\theta\theta\theta}(r, \phi_1, \rho, \phi_1) + G_{\theta\theta\theta}(r, \phi_1, \rho, \phi_1)] d\rho + \dots$$

$$\frac{2\mu}{\pi(\kappa + 1)} \int_0^{l_2} B_r^2(\rho) [F_{r\theta\theta}(r, \phi_1, \rho, \phi_2) + G_{r\theta\theta}(r, \phi_1, \rho, \phi_2)] + B_\theta^2(\rho) [F_{\theta\theta\theta}(r, \phi_1, \rho, \phi_2) + G_{\theta\theta\theta}(r, \phi_1, \rho, \phi_2)] d\rho \dots$$

$$= -K_I f_{\theta\theta}^I(\phi_1) r^{\lambda_I - 1} - K_{II} f_{\theta\theta}^{II}(\phi_1) r^{\lambda_{II} - 1} \quad (37)$$

$$\frac{2\mu}{\pi(\kappa + 1)} \int_0^{l_1} B_r^1(\rho) [F_{rr\theta}(r, \phi_2, \rho, \phi_1) + G_{rr\theta}(r, \phi_2, \rho, \phi_1)] + B_\theta^1(\rho) [F_{\theta r\theta}(r, \phi_2, \rho, \phi_1) + G_{\theta r\theta}(r, \phi_2, \rho, \phi_1)] d\rho + \dots$$

$$\frac{2\mu}{\pi(\kappa + 1)} \int_0^{l_2} B_r^2(\rho) [F_{rr\theta}(r, \phi_2, \rho, \phi_2) + G_{rr\theta}(r, \phi_2, \rho, \phi_2)] + B_\theta^2(\rho) [F_{\theta r\theta}(r, \phi_2, \rho, \phi_2) + G_{\theta r\theta}(r, \phi_2, \rho, \phi_2)] d\rho \dots$$

$$= -K_I f_{r\theta}^I(\phi_2) r^{\lambda_I - 1} - K_{II} f_{r\theta}^{II}(\phi_2) r^{\lambda_{II} - 1} \quad (38)$$

$$\frac{2\mu}{\pi(\kappa + 1)} \int_0^{l_1} B_r^1(\rho) [F_{r\theta\theta}(r, \phi_2, \rho, \phi_1) + G_{r\theta\theta}(r, \phi_2, \rho, \phi_1)] + B_\theta^1(\rho) [F_{\theta\theta\theta}(r, \phi_2, \rho, \phi_1) + G_{\theta\theta\theta}(r, \phi_2, \rho, \phi_1)] d\rho + \dots$$

$$\frac{2\mu}{\pi(\kappa + 1)} \int_0^{l_2} B_r^2(\rho) [F_{r\theta\theta}(r, \phi_2, \rho, \phi_2) + G_{r\theta\theta}(r, \phi_2, \rho, \phi_2)] + B_\theta^2(\rho) [F_{\theta\theta\theta}(r, \phi_2, \rho, \phi_2) + G_{\theta\theta\theta}(r, \phi_2, \rho, \phi_2)] d\rho \dots$$

$$= -K_I f_{\theta\theta}^I(\phi_2) r^{\lambda_I - 1} - K_{II} f_{\theta\theta}^{II}(\phi_2) r^{\lambda_{II} - 1} \quad (39)$$

## Two crack transforms

Firstly, let us assume without loss of generality that  $l_1 \geq l_2$ . Let us define the following transforms

$$\begin{aligned} r &= \frac{l_1}{2}(v+1) & \rho &= \frac{l_1}{2}(u+1) & \text{alternatively} \\ v &= \frac{2r}{l_1} - 1 & u &= \frac{2\rho}{l_1} - 1. \end{aligned} \quad (40)$$

Further note that

$$\frac{d\rho}{du} = \frac{l_1}{2} \quad \text{therefore} \quad d\rho = du \frac{l_1}{2}. \quad (41)$$

Finally we define

$$l_R = \frac{l_2}{l_1}$$

and then define similar transformations relating to crack 2

$$\rho = l_R \frac{l_1}{2}(u+1) \quad \text{alternatively} \quad u = \frac{1}{l_R} \frac{2\rho}{l_1} - 1. \quad (42)$$

Further note that

$$\frac{d\rho}{du} = l_R \frac{l_1}{2} \quad \text{therefore} \quad d\rho = l_R \frac{l_1}{2} du. \quad (43)$$

If we now consider just equation 36 and apply these transformations, we get

$$\begin{aligned} & \int_{-1}^1 \bar{B}_r^1(u) \left[ F_{rr\theta} \left( \frac{l_1}{2}(v+1), \phi_1, \frac{l_1}{2}(u+1), \phi_1 \right) + G_{rr\theta} \left( \frac{l_1}{2}(v+1), \phi_1, \frac{l_1}{2}(u+1), \phi_1 \right) \right] + \dots \\ & \bar{B}_\theta^1(u) \left[ F_{\theta r\theta} \left( \frac{l_1}{2}(v+1), \phi_1, \frac{l_1}{2}(u+1), \phi_1 \right) + G_{\theta r\theta} \left( \frac{l_1}{2}(v+1), \phi_1, \frac{l_1}{2}(u+1), \phi_1 \right) \right] du + \dots \\ & l_R \int_{-1}^1 \bar{B}_r^2(u) \left[ F_{rr\theta} \left( \frac{l_1}{2}(v+1), \phi_1, l_R \frac{l_1}{2}(u+1), \phi_2 \right) + G_{rr\theta} \left( \frac{l_1}{2}(v+1), \phi_1, l_R \frac{l_1}{2}(u+1), \phi_2 \right) \right] + \dots \\ & \bar{B}_\theta^2(u) \left[ F_{\theta r\theta} \left( \frac{l_1}{2}(v+1), \phi_1, l_R \frac{l_1}{2}(u+1), \phi_2 \right) + G_{\theta r\theta} \left( \frac{l_1}{2}(v+1), \phi_1, l_R \frac{l_1}{2}(u+1), \phi_2 \right) \right] du \dots \\ & = -K_I f_{r\theta}^I(\phi_1) \left( \frac{l_1}{2}(v+1) \right)^{\lambda_I-1} - K_{II} f_{r\theta}^{II}(\phi_1) \left( \frac{l_1}{2}(v+1) \right)^{\lambda_{II}-1} \end{aligned} \quad (44)$$

where

$$\bar{B}_i^j(s) = \frac{l_1 \mu}{\pi(\kappa+1)} B_i^j(s).$$

It is important to note that equation 36 is referring to clearing tractions from the interface of crack number 1, and as such, the observation points are defined in relation to crack number 1.

We have previously shown by Burgers vector argument that

$$F_{ijk}(r, \theta, \rho, \phi) = m F_{ijk}(mr, \theta, m\rho, \phi). \quad (45)$$

So making use of this in equation 44

$$\begin{aligned} & \int_{-1}^1 \hat{B}_r^1(u) [F_{rr\theta}(v+1, \phi_1, u+1, \phi_1) + G_{rr\theta}(v+1, \phi_1, u+1, \phi_1)] + \dots \\ & \hat{B}_\theta^1(u) [F_{\theta r\theta}(v+1, \phi_1, u+1, \phi_1) + G_{\theta r\theta}(v+1, \phi_1, u+1, \phi_1)] du + \dots \\ & l_R \int_{-1}^1 \hat{B}_r^2(u) [F_{rr\theta}(v+1, \phi_1, l_R(u+1), \phi_2) + G_{rr\theta}(v+1, \phi_1, l_R(u+1), \phi_2)] + \dots \\ & \hat{B}_\theta^2(u) [F_{\theta r\theta}(v+1, \phi_1, l_R(u+1), \phi_2) + G_{\theta r\theta}(v+1, \phi_1, l_R(u+1), \phi_2)] du \dots \\ & = -K_I f_{r\theta}^I(\phi_1) \left( \frac{l_1}{2}(v+1) \right)^{\lambda_I-1} - K_{II} f_{r\theta}^{II}(\phi_1) \left( \frac{l_1}{2}(v+1) \right)^{\lambda_{II}-1} \end{aligned}$$

where

$$\hat{B}_i^j(u) = \frac{2\mu}{\pi(\kappa+1)} B_i^j(u).$$



So the formulation of equations 36 and 37 becomes

$$\begin{aligned}
& \int_{-1}^1 \hat{B}_r^1(u) [F_{rr\theta}(v+1, \phi_1, u+1, \phi_1) + G_{rr\theta}(v+1, \phi_1, u+1, \phi_1)] + \dots \\
& \hat{B}_\theta^1(u) [F_{\theta r\theta}(v+1, \phi_1, u+1, \phi_1) + G_{\theta r\theta}(v+1, \phi_1, u+1, \phi_1)] du + \dots \\
& l_R \int_{-1}^1 \hat{B}_r^2(u) [F_{rr\theta}(v+1, \phi_1, l_R(u+1), \phi_2) + G_{rr\theta}(v+1, \phi_1, l_R(u+1), \phi_2)] + \dots \\
& \hat{B}_\theta^2(u) [F_{\theta r\theta}(v+1, \phi_1, l_R(u+1), \phi_2) + G_{\theta r\theta}(v+1, \phi_1, l_R(u+1), \phi_2)] du \dots \\
& = -K_I f_{r\theta}^I(\phi_1) \left( \frac{l_1}{2}(v+1) \right)^{\lambda_I-1} - K_{II} f_{r\theta}^{II}(\phi_1) \left( \frac{l_1}{2}(v+1) \right)^{\lambda_{II}-1}
\end{aligned} \tag{46}$$

$$\begin{aligned}
& \int_{-1}^1 \hat{B}_r^1(u) [F_{r\theta\theta}(v+1, \phi_1, u+1, \phi_1) + G_{r\theta\theta}(v+1, \phi_1, u+1, \phi_1)] + \dots \\
& \hat{B}_\theta^1(u) [F_{\theta\theta\theta}(v+1, \phi_1, u+1, \phi_1) + G_{\theta\theta\theta}(v+1, \phi_1, u+1, \phi_1)] du + \dots \\
& l_R \int_{-1}^1 \hat{B}_r^2(u) [F_{r\theta\theta}(v+1, \phi_1, l_R(u+1), \phi_2) + G_{r\theta\theta}(v+1, \phi_1, l_R(u+1), \phi_2)] + \dots \\
& \hat{B}_\theta^2(u) [F_{\theta\theta\theta}(v+1, \phi_1, l_R(u+1), \phi_2) + G_{\theta\theta\theta}(v+1, \phi_1, l_R(u+1), \phi_2)] du \dots \\
& = -K_I f_{\theta\theta}^I(\phi_1) \left( \frac{l_1}{2}(v+1) \right)^{\lambda_I-1} - K_{II} f_{\theta\theta}^{II}(\phi_1) \left( \frac{l_1}{2}(v+1) \right)^{\lambda_{II}-1}
\end{aligned} \tag{47}$$

The other two equations refer to clearing tractions along crack 2. So we will use a new transform

$$r = l_R \frac{l_1}{2}(v+1),$$

thus substitution into equation 38 yields

$$\begin{aligned}
& \int_{-1}^1 \bar{B}_r^1(u) \left[ F_{rr\theta} \left( l_R \frac{l_1}{2}(v+1), \phi_2, \frac{l_1}{2}(u+1), \phi_1 \right) + G_{rr\theta} \left( l_R \frac{l_1}{2}(v+1), \phi_2, \frac{l_1}{2}(u+1), \phi_1 \right) \right] + \dots \\
& \bar{B}_\theta^1(u) \left[ F_{\theta r\theta} \left( l_R \frac{l_1}{2}(v+1), \phi_2, \frac{l_1}{2}(u+1), \phi_1 \right) + G_{\theta r\theta} \left( l_R \frac{l_1}{2}(v+1), \phi_2, \frac{l_1}{2}(u+1), \phi_1 \right) \right] du + \dots \\
& l_R \int_{-1}^1 \bar{B}_r^2(u) \left[ F_{rr\theta} \left( l_R \frac{l_1}{2}v+1, \phi_2, l_R \frac{l_1}{2}(u+1), \phi_2 \right) + G_{rr\theta} \left( l_R \frac{l_1}{2}v+1, \phi_2, l_R \frac{l_1}{2}(u+1), \phi_2 \right) \right] + \dots \\
& \bar{B}_\theta^2(u) \left[ F_{\theta r\theta} \left( l_R \frac{l_1}{2}v+1, \phi_2, l_R \frac{l_1}{2}(u+1), \phi_2 \right) + G_{\theta r\theta} \left( l_R \frac{l_1}{2}v+1, \phi_2, l_R \frac{l_1}{2}(u+1), \phi_2 \right) \right] du \dots \\
& = -K_I f_{r\theta}^I(\phi_2) \left( l_R \frac{l_1}{2}(v+1) \right)^{\lambda_I-1} - K_{II} f_{r\theta}^{II}(\phi_2) \left( l_R \frac{l_1}{2}(v+1) \right)^{\lambda_{II}-1}
\end{aligned} \tag{48}$$

where still

$$\bar{B}_i^j(u) = \frac{l_1 \mu}{\pi(\kappa+1)} B_i^j(u).$$

Further kernel reduction as before gives

$$\begin{aligned}
& \int_{-1}^1 \hat{B}_r^1(u) [F_{rr\theta}(l_R(v+1), \phi_2, u+1, \phi_1) + G_{rr\theta}(l_R(v+1), \phi_2, u+1, \phi_1)] + \dots \\
& \hat{B}_\theta^1(u) [F_{\theta r\theta}(l_R(v+1), \phi_2, u+1, \phi_1) + G_{\theta r\theta}(l_R(v+1), \phi_2, u+1, \phi_1)] du + \dots \\
& \int_{-1}^1 \hat{B}_r^2(u) [F_{rr\theta}(v+1, \phi_2, u+1, \phi_2) + G_{rr\theta}(v+1, \phi_2, u+1, \phi_2)] + \dots \\
& \hat{B}_\theta^2(u) [F_{\theta r\theta}(v+1, \phi_2, u+1, \phi_2) + G_{\theta r\theta}(v+1, \phi_2, u+1, \phi_2)] du \dots \\
& = -K_I f_{r\theta}^I(\phi_2) \left( l_R \frac{l_1}{2}(v+1) \right)^{\lambda_I-1} - K_{II} f_{r\theta}^{II}(\phi_2) \left( l_R \frac{l_1}{2}(v+1) \right)^{\lambda_{II}-1}
\end{aligned}$$

where still

$$\hat{B}_i^j(u) = \frac{2\mu}{\pi(\kappa + 1)} B_i^j(u).$$

So the formulation of equations 38 and 39 becomes equations

$$\begin{aligned} & \int_{-1}^1 \hat{B}_r^1(u) [F_{rr\theta}(l_R(v+1), \phi_2, u+1, \phi_1) + G_{rr\theta}(l_R(v+1), \phi_2, u+1, \phi_1)] + \dots \\ & \hat{B}_\theta^1(u) [F_{\theta r\theta}(l_R(v+1), \phi_2, u+1, \phi_1) + G_{\theta r\theta}(l_R(v+1), \phi_2, u+1, \phi_1)] du + \dots \\ & \int_{-1}^1 \hat{B}_r^2(u) [F_{rr\theta}(v+1, \phi_2, u+1, \phi_2) + G_{rr\theta}(v+1, \phi_2, u+1, \phi_2)] + \dots \\ & \hat{B}_\theta^2(u) [F_{\theta r\theta}(v+1, \phi_2, u+1, \phi_2) + G_{\theta r\theta}(v+1, \phi_2, u+1, \phi_2)] du \dots \\ & = -K_I f_{r\theta}^I(\phi_2) \left( l_R \frac{l_1}{2}(v+1) \right)^{\lambda_I-1} - K_{II} f_{r\theta}^{II}(\phi_2) \left( l_R \frac{l_1}{2}(v+1) \right)^{\lambda_{II}-1} \end{aligned} \quad (49)$$

$$\begin{aligned} & \int_{-1}^1 \hat{B}_r^1(u) [F_{r\theta\theta}(l_R(v+1), \phi_2, u+1, \phi_1) + G_{r\theta\theta}(l_R(v+1), \phi_2, u+1, \phi_1)] + \dots \\ & \hat{B}_\theta^1(u) [F_{\theta\theta\theta}(l_R(v+1), \phi_2, u+1, \phi_1) + G_{\theta\theta\theta}(l_R(v+1), \phi_2, u+1, \phi_1)] du + \dots \\ & \int_{-1}^1 \hat{B}_r^2(u) [F_{r\theta\theta}(v+1, \phi_2, u+1, \phi_2) + G_{r\theta\theta}(v+1, \phi_2, u+1, \phi_2)] + \dots \\ & \hat{B}_\theta^2(u) [F_{\theta\theta\theta}(v+1, \phi_2, u+1, \phi_2) + G_{\theta\theta\theta}(v+1, \phi_2, u+1, \phi_2)] du \dots \\ & = -K_I f_{\theta\theta}^I(\phi_2) \left( l_R \frac{l_1}{2}(v+1) \right)^{\lambda_I-1} - K_{II} f_{\theta\theta}^{II}(\phi_2) \left( l_R \frac{l_1}{2}(v+1) \right)^{\lambda_{II}-1} \end{aligned} \quad (50)$$